CANCER THERAPY

MTAP deletion confers enhanced dependency on the PRMT5 arginine methyltransferase in cancer cells

Gregory V. Kryukov,[1,2]* Frederick H. Wilson,[1,2]* Jason R. Ruth,[1,2]* Joshiawa Paulk,[1,2] Aviad Tsherniak,[2] Sara E. Marlow,[1,2] Francisca Vazquez,[1,2] Barbara A. Weir,[1,2] Mark E. Fitzgerald,[2] Minoru Tanaka,[1,2] Craig M. Bielski,[1,2] Justin M. Scott,[2] Courtney Dennis,[2] Glenn S. Cowley,[2] Jesse S. Boehm,[2] David E. Root,[2] Todd R. Golub,[2] Clary B. Clish,[2] James E. Bradner,[1,2] William C. Hahn,[1,2] Levi A. Garraway[1,2]†

The discovery of cancer dependencies has the potential to inform therapeutic strategies and to identify putative drug targets. Integrating data from comprehensive genomic profiling of cancer cell lines and from functional characterization of cancer cell dependencies, we discovered that loss of the enzyme methylthioadenosine phosphorylase (MTAP) confers a selective dependence on protein arginine methyltransferase 5 (PRMT5) and its binding partner WDR77. MTAP is frequently lost due to its proximity to the commonly deleted tumor suppressor gene, *CDKN2A*. We observed increased intracellular concentrations of methylthioadenosine (MTA, the metabolite cleaved by MTAP) in cells harboring *MTAP* deletions. Furthermore, MTA specifically inhibited PRMT5 enzymatic activity. Administration of either MTA or a small-molecule PRMT5 inhibitor showed a modest preferential impairment of cell viability for MTAP-null cancer cell lines compared with isogenic MTAP-expressing counterparts. Together, our findings reveal PRMT5 as a potential vulnerability across multiple cancer lineages augmented by a common "passenger" genomic alteration.

The gene encoding methylthioadenosine phosphorylase (MTAP) is ubiquitously expressed in normal tissues (fig. S1). However, homozygous deletion of *MTAP* occurs frequently in cancer due to its proximity to *CDKN2A*, one of the most commonly deleted tumor suppressor genes (Fig. 1A) (*1*–*7*). For example, *MTAP* is deleted in 40% of glioblastomas; 25% of melanomas, urothelial carcinomas, and pancreatic adenocarcinomas; and 15% of non–small cell lung carcinomas (NSCLC) (*8*). MTAP cleaves methylthioadenosine (MTA) to generate precursor substrates for methionine and adenine salvage pathways. Synthetic lethal strategies to exploit MTAP loss with methionine starvation or by inhibiting de novo purine synthesis have been proposed; however, clinical efficacy of such approaches has not been demonstrated (*9*–*11*).

We searched for genetic vulnerabilities associated with MTAP loss by leveraging genome-scale pooled short hairpin RNA (shRNA) screening data for 216 cancer cell lines from Project Achilles (*12*, *13*). *MTAP* deletion status for each line was determined using profiles of *MTAP* copy number and mRNA expression from the Cancer Cell Line Encyclopedia (CCLE) (data table S1) (*14*). We correlated 50,529 shRNA sensitivity profiles with *MTAP* deletion status across these lines and identified two shRNAs that strongly correlated with reduced viability of MTAP-null ($MTAP^-$) lines (n = 50) but not MTAP-positive ($MTAP^+$) lines (n = 166) (Fig. 1B and data table S2). One shRNA targeted *PRMT5* (shPRMT5 #1; two-sided Wilcoxon $P < 3 \times 10^{-15}$) and the other targeted *WDR77* (shWDR77 #1; $P < 4 \times 10^{-12}$). We observed a correlation between sensitivity to these shRNAs (Fig. 1C), suggesting that $MTAP^-$ lines sensitive to suppression with either shRNA were generally also sensitive to suppression with the other shRNA. Cell lines with loss of *CDKN2A* but not *MTAP* were generally less sensitive to *PRMT5* or *WDR77* depletion than were lines with codeletion of *CDKN2A* and *MTAP*, suggesting a correlation with *MTAP* (but not *CDKN2A*) loss (Fig. 1D and fig. S2). To provide further support for a possible dependency on *PRMT5* or *WDR77* in the setting of *MTAP* loss, we examined additional shRNAs targeting *PRMT5* and *WDR77* from the screening data set. We identified a second shRNA targeting *PRMT5* (shPRMT5 #2) and *WDR77* (shWDR77 #2) that also demonstrated a strong correlation between impaired cell viability and *MTAP* loss (Fig. 1E and data table S3).

False-positive findings can occur from genome-scale shRNA analyses because of "off-target" microRNA-like effects attributable to partial sequence complementarity with the 5′ end of the shRNA (known as the "seed" region) (*15*, *16*). To investigate this possibility, we identified shRNAs from the screening data set that shared sequence identity in the seed region with each of the four shRNAs targeting *PRMT5* or *WDR77*. None of the shRNAs with shared seed sequence identity demonstrated a correlation between cell viability and MTAP status comparable to that observed for the shRNAs targeting *PRMT5* or *WDR77*, arguing that the differential viability was not caused by a seed effect (fig. S3 and tables S1 and S2). We also confirmed on-target activity of all four shRNAs against *PRMT5* or *WDR77* by immunoblotting of lysates from shRNA-expressing cells (fig. S4).

PRMT5 and *WDR77* encode critical components of the methylosome. PRMT5 forms a complex with WDR77 and catalyzes the transfer of methyl groups to arginine side chains of target proteins, including histones (involved in chromatin remodeling and gene expression) and Sm proteins (RNA-binding proteins involved in mRNA processing) (*17*–*19*). Genetic depletion of PRMT5 has previously been reported to impair cancer cell viability by promoting G1 cell cycle arrest and apoptosis (*20*–*22*). Interestingly, shRNAs targeting either *PRMT5* or *WDR77* reduced levels of both proteins (while demonstrating specific suppression of the target transcript), consistent with depletion of the methylosome complex using either shRNA (fig. S4). $MTAP^-$ cells were also sensitive to shRNA-mediated depletion of *CLNS1A* and *RIOK1*, which encode two additional components of the methylosome (Fig. 1E) (*23*). Finally, the correlation between MTAP loss and sensitivity to *PRMT5* or *WDR77* suppression was not confounded by cell lineage. Within individual lineages (including glioma, pancreatic adenocarcinoma, and NSCLC), $MTAP^-$ cell lines were generally (but not universally) more sensitive to depletion of *PRMT5* and *WDR77* than were $MTAP^+$ lines (Fig. 1F and fig. S2).

Based on these observations, we hypothesized that MTAP loss may confer enhanced sensitivity to genetic suppression of *PRMT5* and *WDR77*. To validate this hypothesis, we examined effects of shRNAs targeting *PRMT5* and *WDR77* on cell viability in 275 additional cancer cell lines profiled through Project Achilles. This profiling data was generated using an expanded shRNA library with additional shRNAs not included in the initial study. Similar to findings from the initial screening data set, we observed that $MTAP^-$ lines (n = 47) were generally more sensitive to *PRMT5* or *WDR77* suppression than $MTAP^+$ lines (n = 228) (Fig. 1G and data table S4). Three of the four shRNAs used to establish our initial finding from the screening data set again demonstrated a strong correlation between loss of cell viability and *MTAP* status, as did an additional shRNA targeting *PRMT5* not included in the screening data set (shPRMT5 #3). In total, the overall increased sensitivity of $MTAP^-$ cells to *PRMT5* or *WDR77* depletion was demonstrated with five shRNAs (three targeting *PRMT5* and two targeting *WDR77*) from two independent functional data sets comprising 491 cancer cell lines (fig. S5).

To determine whether the effects of *PRMT5* or *WDR77* suppression on cell viability are affected by MTAP, we first introduced MTAP into four $MTAP^-$ cell lines [LU99 and H647 (NSCLC), SF-172 (glioma), and SU.86.86 (pancreatic ductal carcinoma)]. This resulted in robust MTAP protein expression in MTAP-reconstituted lines, whereas

[1]Department of Medical Oncology, Dana-Farber Cancer Institute, Harvard Medical School, Boston, MA 02215, USA. [2]The Broad Institute of MIT and Harvard, Cambridge, MA 02142, USA.
*These authors contributed equally to this work. †Corresponding author. E-mail: levi_garraway@dfci.harvard.edu

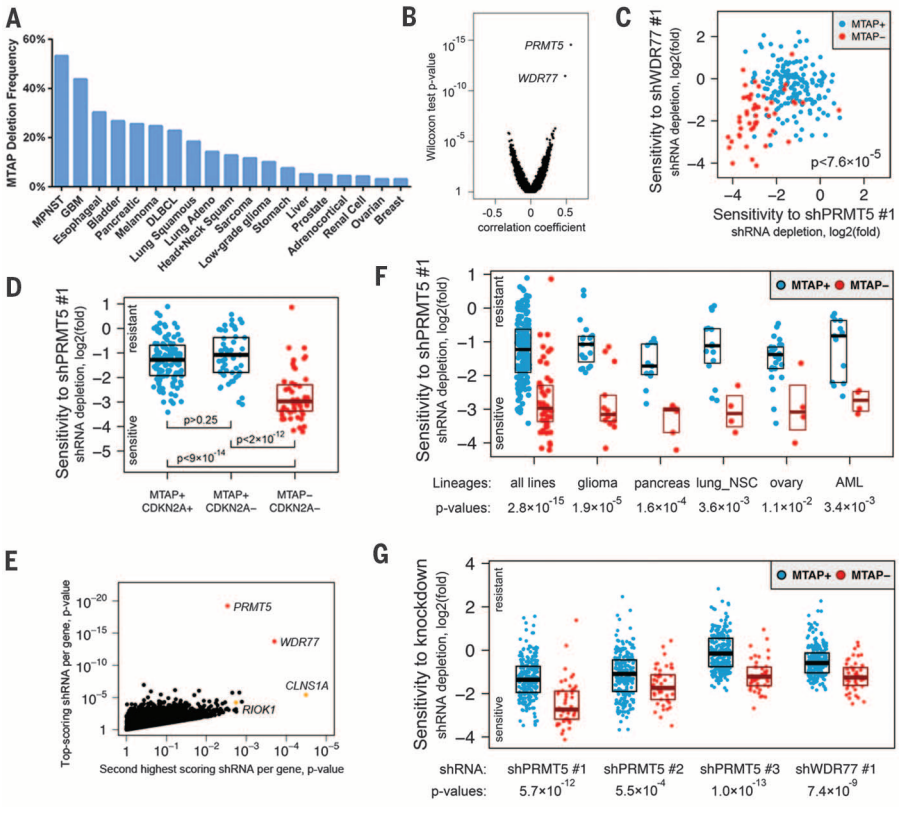

Fig. 1. Cancer cell lines with homozygous *MTAP* loss are selectively sensitive to suppression of *PRMT5* or *WDR77*. (**A**) Frequency of MTAP deletion for selected cancers is shown. Data was obtained from the cBioPortal for Cancer Genomics (http://www.cbioportal.org). MPNST, malignant peripheral nerve sheath tumor; GBM, glioblastoma; DLBCL, diffuse large B cell lymphoma. (**B**) Point biserial correlation coefficients for association with MTAP loss are plotted against Wilcoxon two-class comparison test *P* values for 50,529 shRNAs. (**C**) Log2(fold) of depletion of shPRMT5 #1 and shWDR77 #1 are shown, demonstrating a correlation between sensitivity to these shRNAs for MTAP$^-$ lines. (**D**) Log2(fold) of shPRMT5 #1 depletion is plotted for cell lines with the indicated genotypes. Median with upper and lower 25th percentiles are shown. (**E**) Pearson correlation test *P* values for the top-scoring shRNAs are plotted against *P* values for the second best-scoring shRNAs targeting the same gene. Selective sensitivity of MTAP$^-$ lines to depletion of the methylosome is supported by at least two hairpins targeting four members of the complex, including constitutive members of the complex (PRMT5 and WDR77, red) and mutually exclusive substrate adaptors (CLNS1A and RIOK1, orange). (**F**) Log2(fold) of shPRMT5 #1 depletion is plotted for all 216 cell lines (left) and for lines from the indicated lineages. lung_NSC, non–small cell lung cancer; AML, acute myeloid leukemia. (**G**) Log2(fold) depletion for the indicated shRNAs is shown for all 275 cell lines from the validation cohort.

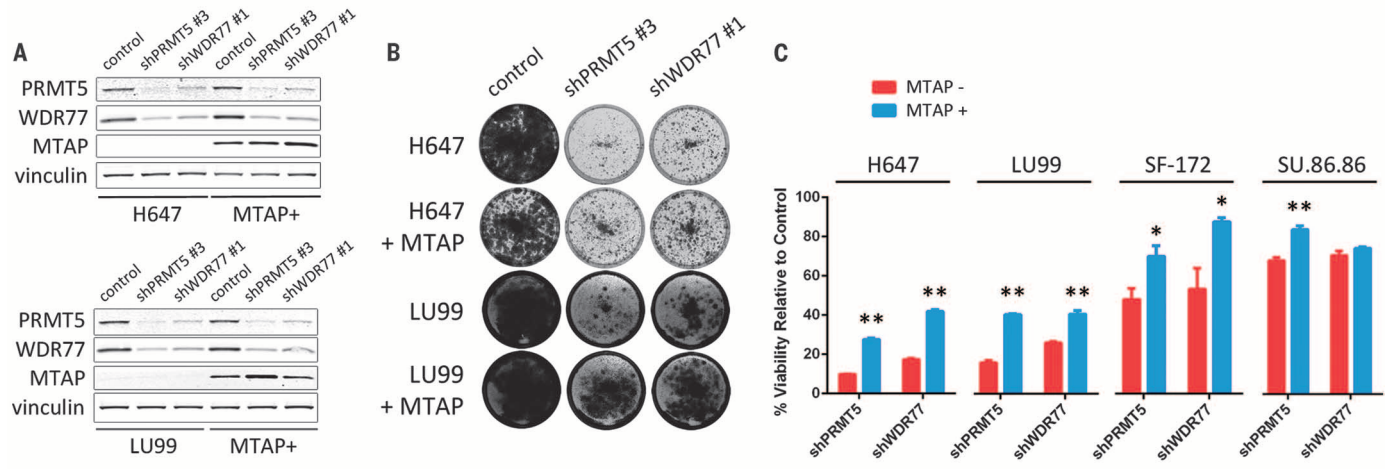

Fig. 2. Cells with MTAP loss are more sensitive to suppression of *PRMT5* and *WDR77* than isogenic MTAP-reconstituted cells. (**A**) Protein lysates were harvested from H647 (top) or LU99 (bottom) and from MTAP-reconstituted H647 or LU99 cells (MTAP$^+$) 5 days after lentiviral transduction with the indicated shRNAs or control. Lysates were fractionated by SDS–polyacrylamide gel electrophoresis (SDS-PAGE), and immunoblotting was performed with the indicated antibodies. (**B**) H647 or LU99 cells and MTAP-reconstituted H647 or LU99 cells were transduced with lentivirus harboring the indicated shRNAs and stained with crystal violet after 10 to 18 days. Media change was performed every 3 days. (**C**) Quantitation of crystal violet uptake by cells transduced with shRNAs targeting *PRMT5* or *WDR77* (normalized to control shRNA for each cell line). Mean and standard error of three to four replicates are shown. The experiment was performed two to three times for each of the four cell line pairs. $^{**}P < 0.01$; $^{*}P < 0.05$ by two-tailed Student's *t* test.

MTAP was absent from parental lines (Fig. 2A and fig. S6). We then performed colony formation assays to assess differences in cell viability after depletion of *PRMT5* or *WDR77* in the presence or absence of MTAP. We observed a reduction in cell viability for each MTAP$^-$ cell line with *PRMT5* or *WDR77* suppression, consistent with our screening and validation results (Fig. 2, B and C and fig. S6). Overall, MTAP-reconstituted lines demonstrated reduced sensitivity to *PRMT5* or *WDR77* suppression compared with isogenic MTAP$^-$ counterparts, suggesting a functional link between MTAP loss and PRMT5 or WDR77 dependency (Fig. 2, B and C and fig. S6).

Previous studies suggest that the activity of PRMT proteins may be inhibited by MTA (the substrate of MTAP) (*24*, *25*). MTA is an analog of S-adenosyl methionine (SAM), the donor substrate for PRMT-mediated methylation (*26*). We hypothesized that somatic *MTAP* loss may lead to increased intracellular MTA concentrations, which

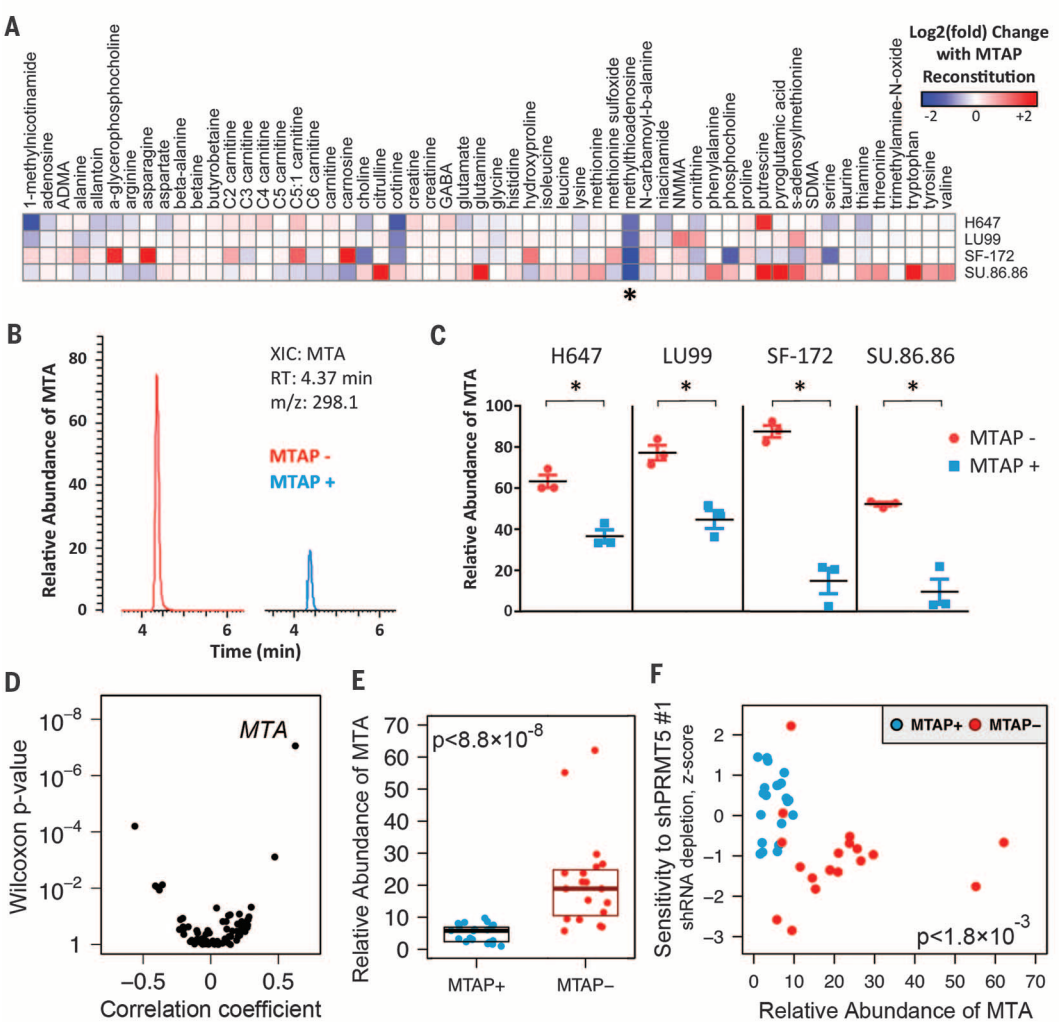

Fig. 3. Intracellular MTA is increased in MTAP$^-$ cells and correlates with sensitivity to *PRMT5* suppression. (**A**) Relative abundance of 56 profiled metabolites was compared for cell extracts from four isogenic cell line pairs. Fold change in relative abundance of each metabolite with MTAP reconstitution is shown for each isogenic pair. Results represent the mean of two independent experiments with three replicates per cell line. Findings for MTA are indicated with an asterisk. (**B**) Representative extracted ion chromatograms (XICs) from LC-MS/MS analysis of SF-172 (left) or MTAP-reconstituted SF-172 (right) cell extracts demonstrating a peak corresponding to MTA. RT, retention time; m/z, mass-to-charge ratio. (**C**) Relative abundance of MTA from cell extracts is displayed. Mean and standard error of three biological replicates are shown. The experiment was performed twice with similar findings. *$P < 0.01$ by Student's t test. (**D**) Correlation of metabolite levels with MTAP loss is shown. Point biserial correlation coefficients are plotted against Wilcoxon two-class comparison test P values for 73 metabolites profiled across 40 MTAP$^+$ and MTAP$^-$cell lines. (**E**) Relative abundance of MTA from MTAP$^+$ (n = 21) and MTAP$^-$ (n = 19) cell lines from various lineages is shown. For each cell line, mean of three biological replicates is displayed. Median with upper and lower 25th percentiles are shown for MTAP$^-$ and MTAP$^+$ lines. (**F**) Correlation of intracellular MTA levels with sensitivity to *PRMT5* depletion is shown. shPRMT5 sensitivity data from the screening and validation studies was normalized and combined using modified z scores. Z scores are plotted against relative intracellular abundance of MTA for the 40 assayed cell lines. Spearman rank correlation P value is shown.

in turn confers a partial inhibition of PRMT5 activity. Together, these effects may heighten cell sensitivity to further reductions in PRMT5 activity (e.g., through genetic suppression). To test this hypothesis, we first determined whether MTAP$^-$ cells contain elevated MTA levels. We used liquid chromatography tandem mass spectrometry (LC-MS/MS) to quantify levels of 56 metabolites (including MTA) from LU99, H647, SF-172, and SU.86.86 cells and their isogenic MTAP-reconstituted counterpart lines. The abundance of most measured metabolites was not significantly altered by ectopic MTAP expression (Fig. 3A). However, intracellular MTA abundance was reduced by a factor of 1.5 to 6, with MTAP reconstitution in each isogenic cell line pair, consistent with increased intracellular MTA in the absence of MTAP (Fig. 3, A to C).

To determine whether MTA levels are generally higher in MTAP$^-$ cell lines compared with MTAP$^+$ lines, we quantified intracellular levels of 73 metabolites from MTAP$^-$ (n = 19) and MTAP$^+$ (n = 21) cancer cell lines from various lineages, including NSCLC, melanoma, and breast. Among profiled metabolites, the abundance of MTA was most strongly correlated with MTAP loss (Fig. 3D and data tables S5 and S6). We observed an approximately 3.3-fold increase in median MTA levels in MTAP$^-$ lines compared with MTAP$^+$, consistent with the hypothesis that MTAP loss leads to increased intracellular MTA (Fig. 3E). In contrast, intracellular levels of the methyl donor SAM were not significantly different between MTAP$^-$ and MTAP$^+$ lines (fig. S7). Using shRNA sensitivity data from Project Achilles, we also observed a significant correlation between MTA levels and PRMT5 dependency across profiled cell lines (Fig. 3F, fig. S7, and data table S7).

Next, we assessed whether elevated MTA might inhibit PRMT5 activity. PRMT5 catalyzes the formation of symmetric dimethyl arginine (sDMA), whereas most other PRMTs generate asymmetric dimethyl arginine (aDMA) (*17*, *27*, *28*). Using an antibody previously shown to recognize sDMAs generated by PRMT5 (*29*), we observed decreased sDMA levels in MTAP$^-$ cells compared with isogenic, MTAP-reconstituted lines (Fig. 4A). In addition, reduced sDMA was observed in MTAP-reconstituted cells exposed to exogenous MTA, consistent with inhibition of PRMT5 enzymatic activity (Fig. 4A). Similar findings were observed with an antibody recognizing symmetric methylation of histone H4 arginine 3 (H4R3), an established substrate of PRMT5 (Fig. 4A) (*30*). In contrast, we observed only modest effects of MTAP status or exogenous MTA on levels of aDMA (Fig. 4A).

This finding raised the possibility that among PRMT family members, PRMT5 may exhibit heightened sensitivity to MTA intracellular concentrations. To investigate this, we measured the ability of MTA to inhibit the catalytic function of 31 histone methyltransferases (including PRMT5 and the PRMT5/WDR77 complex), using a radioisotope filter binding assay (data table S8) (*31*). We observed more than 100-fold

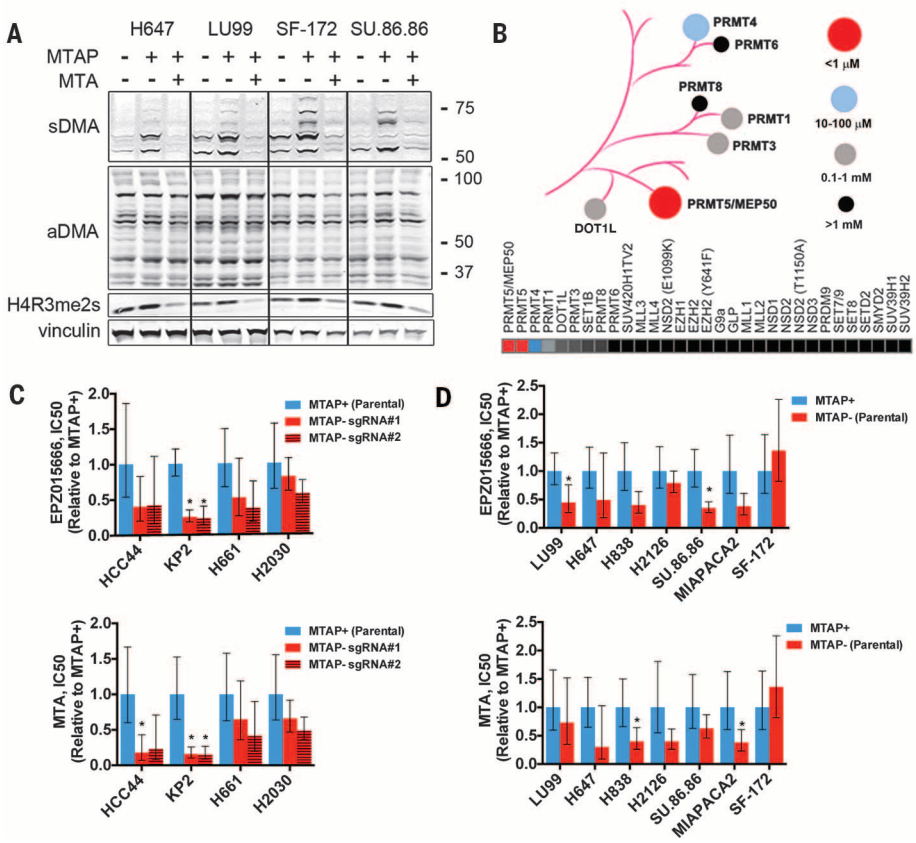

Fig. 4. Pharmacological inhibition of PRMT5. (**A**) Cells were exposed to dimethyl sulfoxide or 200 μM MTA for 48 hours. Lysates were harvested and fractionated by SDS-PAGE. Immunoblotting was performed with the indicated antibodies [recognizing symmetric or asymmetric dimethyl arginine motifs (sDMA and aDMA, respectively), symmetric dimethyl histone H4 arginine 3 (H4R3me2s), or vinculin (loading control)]. Molecular weight is indicated on the right in kDa. (**B**) Dendrogram and heat map indicating relative sensitivity of 31 histone methyltransferases to inhibition by MTA, as determined by radioisotope filter binding assay. (**C** and **D**) Relative cell viability IC_{50} (normalized to $MTAP^+$ cells for each line) for cells treated with EPZ015666 (top) or MTA (bottom), for isogenic cell lines derived from (C) MTAP-expressing parental cell lines or (D) $MTAP^-$ parental cell lines. Mean IC_{50} and 95% confidence interval of six replicates are shown for each cell line. Each experiment was performed twice for each cell line. *$P < 0.05$ by two-tailed Student's *t* test (versus $MTAP^+$ cells).

selectivity for MTA against both PRMT5 and PRMT5/WDR77 activity compared with all other profiled methyltransferases, consistent with the hypothesis that PRMT5 function is selectively vulnerable to elevated MTA concentrations (Fig. 4B). Furthermore, we demonstrated that MTA is a SAM-competitive inhibitor of PRMT5 (fig. S8).

Next, we sought to determine whether $MTAP^-$ cell lines might exhibit increased sensitivity to pharmacologic inhibition of PRMT5 compared with $MTAP^+$ lines. We identified two inhibitors with distinct PRMT5 binding sites: the metabolite MTA itself and EPZ015666, a potent peptide-competitive and SAM-cooperative inhibitor with >10,000-fold specificity against PRMT5 relative to other methyltransferases (*32*). We tested the ability of these inhibitors to selectively impair viability of parental $MTAP^-$ cell lines compared with isogenic lines expressing MTAP, as well as parental $MTAP^+$ cell lines compared with isogenic CRISPR-mediated MTAP knockout lines (fig. S9). Among the 11 isogenic cell line pairs assayed, the IC_{50} values (concentrations of inhibitor that led to a 50% reduction in activity) for $MTAP^-$ cell lines treated with MTA or EPZ015666 were generally lower than IC_{50} values for isogenic $MTAP^+$ lines, consistent with our findings from genetic depletion of *PRMT5* (although with a smaller effect size) (Fig. 4, C and D). Although the results for any given cell line pair were consistent using either PRMT5 inhibitor (fig. S9), the differences between each isogenic cell line pair were generally modest and more pronounced for some pairs than others (the differential sensitivity was absent altogether in SF-172). Furthermore, we did not observe significant differences in mean IC_{50} values between $MTAP^+$ and $MTAP^-$ cell lines for either compound (fig. S9).

The discrepancy in effect size that we observed between genetic depletion and enzymatic inhibition of PRMT5 may be caused by several factors. For example, it is possible that the reported SAM-cooperative mechanism of action of EPZ015666 limits inhibition of PRMT5 in the setting of excess MTA and reduced SAM binding (*32*). Consistent with this, excess MTA is reported to increase the IC_{50} of EPZ015666 by an order of magnitude in assays of PRMT5 activity (*33*). In addition, we cannot exclude the possibility that a noncatalytic PRMT5 function also contributes to the dependency. In this case, therapeutic approaches to exploit this type of vulnerability may require strategies that deplete protein levels of either PRMT5 itself or the larger methylosome complex. Further work will be necessary to explore these and other mechanistic possibilities.

Collectively, our findings suggest that MTAP loss leads to increased intracellular MTA, which in turn inhibits PRMT5 activity and confers heightened susceptibility to further depletion of PRMT5 (fig. S10). Although PRMT5 has recently emerged as a possible therapeutic target in some cancers (*26*), genetic alterations correlated with sensitivity to PRMT5 inhibition have not previously been identified. Our data suggest that many $MTAP^-$ tumors are more sensitive to depletion of the methylosome, although there is an overlapping distribution of sensitivities to *PRMT5* or *WDR77* suppression between $MTAP^-$ and $MTAP^+$ cell lines (Fig. 1, D, F, and G). Thus, MTAP status alone is not sufficient to distinguish cell lines that are sensitive to PRMT5 inhibition. These observations suggest the presence of other modifiers of sensitivity to methylosome depletion that function in a manner independent of *MTAP* status. Nevertheless, our results endorse the unexpected notion that MTAP loss confers sensitivity to PRMT5 depletion. More generally, these findings highlight the value of comprehensive functional and molecular characterization of large cancer cell line collections to promote identification of potentially targetable dependencies conferred by common genetic lesions.

REFERENCES AND NOTES

1. T. Nobori *et al.*, *Proc. Natl. Acad. Sci. U.S.A.* **93**, 6203–6208 (1996).
2. Z. H. Chen, H. Zhang, T. M. Savarese, *Cancer Res.* **56**, 1083–1090 (1996).
3. P. B. Illei, V. W. Rusch, M. F. Zakowski, M. Ladanyi, *Clin. Cancer Res.* **9**, 2108–2113 (2003).
4. S. R. Hustinx *et al.*, *Cancer Biol. Ther.* **4**, 90–93 (2005).
5. E. L. Powell *et al.*, *Am. J. Surg. Pathol.* **29**, 1497–1504 (2005).
6. C. A. Karikari *et al.*, *Mol. Cancer Ther.* **4**, 1860–1866 (2005).
7. S. A. Christopher, P. Diegelman, C. W. Porter, W. D. Kruger, *Cancer Res.* **62**, 6639–6644 (2002).
8. E. Cerami *et al.*, *Cancer Discov.* **2**, 401–404 (2012).
9. J. R. Bertino, W. R. Waud, W. B. Parker, M. Lubin, *Cancer Biol. Ther.* **11**, 627–632 (2011).
10. H. L. Kindler, H. A. Burris 3rd, A. B. Sandler, I. A. Oliff, *Invest. New Drugs* **27**, 75–81 (2009).
11. P. N. Munshi, M. Lubin, J. R. Bertino, *Oncologist* **19**, 760–765 (2014).
12. H. W. Cheung *et al.*, *Proc. Natl. Acad. Sci. U.S.A.* **108**, 12372–12377 (2011).
13. G. S. Cowley *et al.*, *Scientific Data* **1**, 140035 (2014).
14. J. Barretina *et al.*, *Nature* **483**, 603–607 (2012).
15. A. L. Jackson *et al.*, *RNA* **12**, 1179–1187 (2006).
16. F. D. Sigoillot *et al.*, *Nat. Methods* **9**, 363–366 (2012).
17. V. Karkhanis, Y. J. Hu, R. A. Baiocchi, A. N. Imbalzano, S. Sif, *Trends Biochem. Sci.* **36**, 633–641 (2011).
18. W. J. Friesen *et al.*, *Mol. Cell. Biol.* **21**, 8289–8300 (2001).
19. W. J. Friesen *et al.*, *J. Biol. Chem.* **277**, 8243–8247 (2002).

20. A. Scoumanne, J. Zhang, X. Chen, *Nucleic Acids Res.* **37**, 4965–4976 (2009).
21. J. H. Lim *et al.*, *Biochem. Biophys. Res. Commun.* **452**, 1016–1021 (2014).
22. C. M. Koh *et al.*, *Nature* **523**, 96–100 (2015).
23. G. Guderian *et al.*, *J. Biol. Chem.* **286**, 1976–1986 (2011).
24. M. T. Bedford, S. Richard, *Mol. Cell* **18**, 263–272 (2005).
25. H. G. Williams-Ashman, J. Seidenfeld, P. Galletti, *Biochem. Pharmacol.* **31**, 277–288 (1982).
26. Y. Yang, M. T. Bedford, *Nat. Rev. Cancer* **13**, 37–50 (2013).
27. T. L. Branscombe *et al.*, *J. Biol. Chem.* **276**, 32971–32976 (2001).
28. B. P. Pollack *et al.*, *J. Biol. Chem.* **274**, 31531–31542 (1999).
29. F. Liu *et al.*, *J. Clin. Invest.* **125**, 3532–3544 (2015).
30. Q. Zhao *et al.*, *Nat. Struct. Mol. Biol.* **16**, 304–311 (2009).
31. K. Y. Horiuchi *et al.*, *Assay Drug Dev. Technol.* **11**, 227–236 (2013).
32. E. Chan-Penebre *et al.*, *Nat. Chem. Biol.* **11**, 432–437 (2015).
33. K. J. Mavrakis *et al.*, *Science* **351**, aad5944 (2016).

ACKNOWLEDGMENTS

Data from Project Achilles and the Cancer Cell Line Encyclopedia can be accessed at www.broadinstitute.org/achilles and www.broadinstitute.org/ccle/home, respectively. We thank members of the Garraway laboratory for helpful discussion. We thank D. Hernandez for assistance with seeding cell lines for metabolomics studies. We gratefully acknowledge the Carlos Slim Foundation for providing access to shRNA screening data (funded in part by the Slim Initiative in Genomic Medicine for the Americas project) for validation studies. Funding for this work was provided by the Novartis Institutes for BioMedical Research, the Dr. Miriam and Sheldon G. Adelson Medical Research Foundation, the Melanoma Research Alliance, a NIH PO1 Research Program Project grant (each to L.A.G.), an Integrative Cancer Biology Program grant (U54 CA112962 to T.R.G.), and an NIH U01 CA176058 (to W.C.H.). F.H.W. is supported by a Conquer Cancer Foundation of the American Society of Clinical Oncology Young Investigator Award, the 2014 AACR-Bristol-Myers Squibb Oncology Fellowship in Clinical Cancer Research (grant 14-40-15-WILS), a grant from the Karin Grunebaum Cancer Research Foundation, and a KL2/Catalyst Medical Research Investigator Training award (an appointed KL2 award) from Harvard Catalyst/The Harvard Clinical and Translational Science Center (National Center for Research Resources and the National Center for Advancing Translational Sciences, NIH Award KL2 TR001100). G.V.K., A.T., F.V., B.A.W., and C.M.B. performed computational analysis of data sets generated from Project Achilles and CCLE under the supervision of J.S.B., T.R.G., W.C.H., and L.A.G. G.S.C., D.E.R., and W.C.H. supervised the generation of Project Achilles screening data. F.H.W. and S.E.M. performed experiments to validate the computational shRNA screening findings. G.V.K., F.H.W., S.E.M., J.M.S., C.D., and C.B.C. performed metabolomic studies and analyzed data. Isogenic cell line pairs were generated and characterized by F.H.W. and J.R.R. J.R.R. conducted cell viability IC_{50} experiments and the MTA methyltransferase selectivity assay. J.P. performed the MTA mechanism of action study under the supervision of J.E.B. M.E.F. and M.T. synthesized EPZ015666 under the supervision of J.E.B. F.H.W., G.V.K., J.R.R., and L.A.G. wrote the manuscript. L.A.G. is a paid consultant for Novartis and Boehringer Ingelheim; he holds equity in, and is a paid consultant for, Foundation Medicine; and he is a recipient of a grant from Novartis. W.C.H. is a paid consultant for Novartis and recipient of a grant from Novartis. M.T. is a visiting scientist from Mitsubishi Tanabe Pharma Corporation (MTPC) and a recipient of nonresearch support from MTPC. The Broad Institute and the authors (L.A.G., F.H.W., G.V.K., and J.R.R.) have filed a patent application (BI2015/040 46783.00.2109 US PRO Pending 62/131,825) relating to the use of PRMT5 inhibitors to treat MTAP-deficient tumors.

SUPPLEMENTARY MATERIALS

www.sciencemag.org/content/351/6278/1214/suppl/DC1
Materials and Methods
Figs. S1 to S10
Tables S1 and S2
Data Tables S1 to S8
References

7 October 2015; accepted 1 February 2016
Published online 11 February 2016
10.1126/science.aad5214

TRANSCRIPTION

Measurement of gene regulation in individual cells reveals rapid switching between promoter states

Leonardo A. Sepúlveda,[1,2] Heng Xu,[1,2] Jing Zhang,[1,2] Mengyu Wang,[1,2,3] Ido Golding[1,2,3,4]*

In vivo mapping of transcription-factor binding to the transcriptional output of the regulated gene is hindered by probabilistic promoter occupancy, the presence of multiple gene copies, and cell-to-cell variability. We demonstrate how to overcome these obstacles in the lysogeny maintenance promoter of bacteriophage lambda, P_{RM}. We simultaneously measured the concentration of the lambda repressor CI and the number of messenger RNAs (mRNAs) from P_{RM} in individual *Escherichia coli* cells, and used a theoretical model to identify the stochastic activity corresponding to different CI binding configurations. We found that switching between promoter configurations is faster than mRNA lifetime and that individual gene copies within the same cell act independently. The simultaneous quantification of transcription factor and promoter activity, followed by stochastic theoretical analysis, provides a tool that can be applied to other genetic circuits.

Sequence-specific transcription factors drive the diversity of cell phenotypes in development and homeostasis (*1*). For each target gene, alternative transcription-factor binding configurations (by different transcription factors or by multiple copies of the same one) result in varied transcriptional outputs, in turn leading to alternative cell fates and behaviors (*2*, *3*). Elucidating the relations between transcription-factor configurations [which can number in the hundreds (*4*–*6*)] and the resulting transcriptional activity remains a challenge. Application of traditional genetic and biochemical approaches usually requires a genetically modified system or assays of purified components in vitro (*7*). Ideally, however, one would like to map transcription-factor configuration to promoter activity inside the cell, with minimal perturbation to the endogenous system.

Multiple factors hinder such direct measurement. First, individual cells vary in both transcription-factor concentration and the resulting transcriptional activity (*8*, *9*); averaging over many cells thus filters out details of the regulatory relation. Second, even within the single cell, more than one copy of the regulated gene is typically present, with each copy individually regulated (*10*). Finally, even at the level of a single gene copy, multiple binding configurations are possible at a given transcription-factor concentration (*11*, *12*). The relative probabilities of these different configurations and the rate of switching between them will define the stochastic activity of the regulated promoter (*13*).

We simultaneously measured, in individual cells, the concentration of a transcription factor and the number of mRNAs produced from the regulated gene. We also measured how the gene copy number changes through the cell cycle. We then analyzed the full single-cell data using a theoretical model, which allowed us to identify the contributions of different transcription-factor binding configurations to the stochastic activity of the promoter.

Specifically, we examined the lysogeny maintenance promoter of phage lambda, P_{RM}. The regulation of this promoter by its own gene product, the lambda repressor (CI), is a paradigm for how alternative binding configurations drive transcriptional activity and the resulting cell fate—stable lysogeny or lytic induction resulting in cell death (*7*). The number of possible CI configurations is very large [>100 (*4*, *5*)]. Briefly, as CI concentration increases, CI dimers gradually occupy three proximal ($O_{R1\text{-}3}$) and three distal ($O_{L1\text{-}3}$) operator sites, leading first to activation, then repression, of P_{RM} (Fig. 1A). Cooperative CI binding, and looping of DNA between the O_R and O_L sites, play important roles in shaping the P_{RM}(CI) regulatory curve (*14*).

In a lysogen (a bacterium carrying a prophage), CI concentration is believed to be such that P_{RM} fluctuates between the activated and repressed states (*15*) (Fig. 1A), and this has been suggested to stabilize the lysogenic state against random fluctuations in CI levels (*14*). However, the nature of the lysogenic "mixed state" (activated/repressed) is unknown: Are the promoter fluctuations slow

[1]Verna and Marrs McLean Department of Biochemistry and Molecular Biology, Baylor College of Medicine, Houston, TX 77030, USA. [2]Center for Theoretical Biological Physics, Rice University, Houston, TX 77005, USA. [3]Graduate Program in Structural and Computational Biology and Molecular Biophysics, Baylor College of Medicine, Houston, TX 77030, USA. [4]Center for the Physics of Living Cells, University of Illinois at Urbana–Champaign, Urbana, IL 61801, USA.
***Corresponding author. E-mail: golding@bcm.edu; igolding@illinois.edu**

MTAP deletion confers enhanced dependency on the PRMT5 arginine methyltransferase in cancer cells

Gregory V. Kryukov, Frederick H. Wilson, Jason R. Ruth, Joshiawa Paulk, Aviad Tsherniak, Sara E. Marlow, Francisca Vazquez, Barbara A. Weir, Mark E. Fitzgerald, Minoru Tanaka, Craig M. Bielski, Justin M. Scott, Courtney Dennis, Glenn S. Cowley, Jesse S. Boehm, David E. Root, Todd R. Golub, Clary B. Clish, James E. Bradner, William C. Hahn and Levi A. Garraway (February 11, 2016)

Science **351** (6278), 1214-1218. [doi: 10.1126/science.aad5214] originally published online February 11, 2016

Editor's Summary

Tumors put in a vulnerable position

Cancer cells often display alterations in metabolism that help fuel their growth. Such metabolic "rewiring" may also work against the cancer cells, however, by creating new vulnerabilities that can be exploited therapeutically. A variety of human tumors show changes in methionine metabolism caused by loss of the gene coding for 5-methylthioadenosine phosphorylase (MTAP). Mavrakis *et al.* and Kryukov *et al.* found that the loss of MTAP renders cancer cell lines sensitive to growth inhibition by compounds that suppress the activity of a specific arginine methyltransferase called PRMT5. Conceivably, drugs that inhibit PRMT5 activity could be developed into a tailored therapy for MTAP-deficient tumors.

Science, this issue pp. 1208 and 1214

Science (print ISSN 0036-8075; online ISSN 1095-9203) is published weekly, except the last week in December, by the American Association for the Advancement of Science, 1200 New York Avenue NW, Washington, DC 20005.